Journal of Inorganic Biochemistry 244 (2023) 112236

Contents lists available at ScienceDirect

Journal of Inorganic Biochemistry

journal homepage: www.elsevier.com/locate/jinorgbio

^{19}F: A small probe for a giant protein

Lucrezia Cosottini [a,b], Stefano Zineddu [a,b,1], Lara Massai [b], Veronica Ghini [a,b], Paola Turano [a,b,c,*]

[a] Magnetic Resonance Center (CERM), University of Florence, via Luigi Sacconi 6, Sesto Fiorentino 50019, Italy
[b] Department of Chemistry "Ugo Schiff", University of Florence, via della Lastruccia 3, Sesto Fiorentino 50019, Italy
[c] Consorzio Interuniversitario Risonanze Magnetiche di Metallo Proteine (CIRMMP), via Luigi Sacconi 6, Sesto Fiorentino 50019, Italy

ARTICLE INFO

Keywords:
Human ferritin
^{19}F NMR
Nanocage
5-F-Trp
ESI-MS

ABSTRACT

Herein we describe a method for the efficient production (~90% fluorination) of 5-F-Trp human H ferritin via the selective incorporation of ^{19}F into the side chain of W93 using 5-fluoroindole as the fluorinated precursor of the amino acid. Human H ferritin is a nanocage composed of 24 identical subunits, each containing a single Trp belonging to a loop exposed on the external surface of the protein nanocage. This makes 5-F-Trp a potential probe for the study of intermolecular interactions in solution by exploiting its intrinsic fluorescence. More interestingly, albeit the large size of the cage (12 nm external diameter, ~500 kDa molecular mass) we observe a broad but well defined NMR ^{19}F resonance that can be used for the dual purpose of detecting solution intermolecular interactions via chemical shift perturbation mapping and monitoring the uptake of ferritin by cells treated with ferritin-based drug carriers, the latter being an application area of increasing importance.

In this Communication, we present the encounter between two chemical entities: fluorine, which is one of the smallest atoms of the periodic table, and ferritin, which is one of the largest proteins of bioinorganic relevance.

Fluorine has an atomic radius of 0.64 Å and a van der Waals radius of 1.47 Å, both of which make it a good substitute for hydrogen. Its nuclide, ^{19}F, has interesting NMR properties: 100% natural abundance, $I = 1/2$ and high gyromagnetic ratio ($\gamma = 25.18\ 10^7$ rad T^{-1} s^{-1}). The resulting high relative sensitivity (83.3% vs. ^{1}H) and the lack of naturally occurring fluorinated compounds make it a valuable probe. Incorporation of fluorinated amino acids in proteins is receiving growing interest for its broad use in solution, solid-state and in-cell NMR experiments, as nicely reviewed by A. Gronenborn [1]. ^{19}F chemical shift is very sensitive to its environment, so its incorporation into proteins becomes very useful for the monitoring of intermolecular interactions and conformational changes, although the contributions to the chemical shift are not fully theoretically interpretable. As suggested by the same author: "*To make progress toward a more thorough understanding, we need to populate a database of fluorinated protein structures alongside the experimentally measured ^{19}F chemical shifts, interfaced with theory-based computational efforts*" [1].

The second actor in our system is recombinant human H ferritin (HuHf, hereafter), a homopolymeric nanocage of about 500 kDa [2,3] (Fig. 1). After the discovery that ferritins with abundance of H-chains are recognized by Transferrin Receptor 1 (TfR1), which is overexpressed on the surface of many cancer cells [4,5], recombinant human H-ferritin has been increasingly used as a nanocarrier for targeted drug delivery [6–8]. Ferritin is a multifunctional nanoplatform; its internal cavity is optimal to host different chemical entities (from small organic and inorganic molecules to biominerals) and can be easily functionalized on the external surface with a variety of metal ions, fluorophores, polymers, peptides, etc. [8–12]. Additionally, HuHf is stable at high temperature and extreme pH (conditions that expand the range of possible procedures for efficient encapsulation and surface modification). Finally, it is reported to be a biocompatible system with low immunogenicity [13].

^{19}F can be easily incorporated at specific labelling sites, such as Trp residues [14,15]. Each human-H subunit has a single tryptophan (W93) on the solvent exposed BC-loop, for a total of 24 Trp residues for protein

Abbreviations: ESI-MS, Electrospray Ionization Mass Spectrometry; HuHf, Human Heavy chain Ferritin; IPTG, Isopropyl β-D-thiogalactoside; NMR, Nuclear Magnetic Resonance; NOESY, Nuclear Overhauser Effect Spectroscopy; SCARA-5, Scavenger Receptor Class A Member 5; S/N, Signal to Noise ratio; TfR1, Transferrin Receptor-1; WT, Wild Type.

* Corresponding author at: Magnetic Resonance Center (CERM), University of Florence, via Luigi Sacconi 6, Sesto Fiorentino 50019, Italy.
E-mail address: paola.turano@unifi.it (P. Turano).

[1] S.Z. contributed to this work before the start of his PhD.

https://doi.org/10.1016/j.jinorgbio.2023.112236
Received 10 February 2023; Received in revised form 11 April 2023; Accepted 18 April 2023
Available online 23 April 2023

cage [16] **(**Fig. 1B **and Table S1)**. Ferritin labelling was achieved by selective incorporation of ^{19}F into the side chains of Trp residues exploiting a fluorinated precursor (5-fluoroindole), that successfully generates the 5-F-Trp derivative, Scheme 1 [17,18].

The fluorinated recombinant homopolymeric human-H ferritin (^{19}F-HuHf) was expressed in *E. coli* cells by adapting the established protocol for wild type (WT) ferritin production [3,19]. Briefly, the pEt-9a plasmid bearing the human-H ferritin gene, was transformed into BL21(DE3)-pLysS *E. coli* cells. Bacteria were grown in a M9 minimal medium at 37 °C until the $OD_{600\ nm}$ reached a value of 0.6–0.8. Then, 5-fluoroindole was added to the culture with a final concentration of 60 mg/L and incubated for 15′ before the induction of ferritin overexpression with 1 mM IPTG followed by an overnight growth at 25 °C. The purification of the protein was performed by heating of the cell lysate at 65 °C for 15′ and through two consecutive chromatographic steps i.e., anionic exchange and size exclusion chromatography. With this protocol the overall yield of protein production increased up to 89 mg/L with a 90% purity (compared to an average yield of 40 mg/L for the expression of WT in rich medium). In Fig. 2A the size exclusion chromatography shows that ^{19}F-HuHf has the same elution pattern of the WT protein, with a single peak referable to the 24mer assembled cage, thus indicating its correct self-assembly. Far-UV circular dichroism confirmed the correct folding in terms of secondary structure **(**Fig. 2B**)**. The labeling efficiency was estimated via ESI-MS **(**Fig. 2C **and Figs. S1)**, which measures single subunits [20], demonstrating the optimal performance of the adopted protocol with almost 90% of ^{19}F-labeled chains. This result is in line with literature data reporting an incorporation efficiency of the order of 80–95% for the expression of other proteins in *E. coli*. [17,18].

As already reported [21–24], the highly symmetric structure of homopolymeric ferritins represents an obvious simplification for their NMR spectra, where the number of detectable signals equals that expected for a single subunit. Instead, the high molecular mass causes very short T_2 and large linewidths. Thus, ^{1}H resonances display linewidth beyond detection, while signals of reasonable linewidths can be retrieved for low-gyromagnetic nuclei such ^{13}C. The state-of-the-art experiment for the detection of ferritin side chains in solution is the

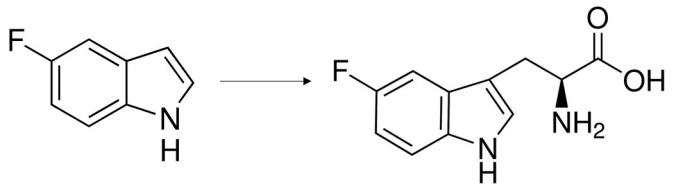

Scheme 1. Structure of 5-fluoroindole (left) and of 5-fluoro-tryptophan (right).

^{13}C-^{13}C NOESY experiment [21–26], which gains intensity due to the long tumbling time and relatively long T_1 values associated to the 12-nm cage. Here, we use 5-F-Trp HuHf to demonstrate that ^{19}F NMR of ferritin is feasible, despite its size. Spectra were acquired at 298 K on a Bruker Avance III spectrometer operating at 14.1 Tesla equipped with a SEL ^{1}H High Power 5 mm probe, using a zg pulse sequence, with a recycle time of 3 s and an acquisition time of 0.57 s. ^{19}F-HuHf gives rise to a broad resonance at −126.12 ppm, with a linewidth of about 700 Hz (**Fig. S2**), with respect to a linewidth of 25 Hz of the free ^{19}F-5-fluoroindole (Fig. 3A). The lower limit of detection was determined by recording spectra at different concentrations; with our experimental settlement it is of the order of 5 μM in cage concentration (Fig. 3A).

Additionally, 5-F-Trp is a useful fluorescent probe [27]. While the absorbance spectrum of ^{19}F-HuHF is essentially superimposable to the reference spectrum of the WT protein, ^{19}F-HuHf features highly enhanced fluorescence with a slightly red shifted emission (λ_{exc} 295 nm, λ_{em} 334 nm) with respect to the intrinsic fluorescence emission of HuHf (λ_{exc} 295 nm, λ_{em} 327 nm), Fig. 2D. While tryptophan decays from its fluorescent excited state via multiple pathways, 5-F-Trp exhibits monoexponential decay kinetics, which simplifies the analysis [28], conferring a consequent higher quantum yield [29]; but the sensitivity of the fluorescence wavelength to the environment solvent polarity is essentially the same as that of Trp [29]. Therefore, 5-F-Trp incorporated in HuHf can be a useful tool for monitoring the interaction of ferritin with partner molecules or characterizing the conformational changes occurring in specific protein variants/derivatives.

^{19}F NMR signals have been proposed as sensitive reporters of the local environment, with a large chemical shift dynamic range (~400

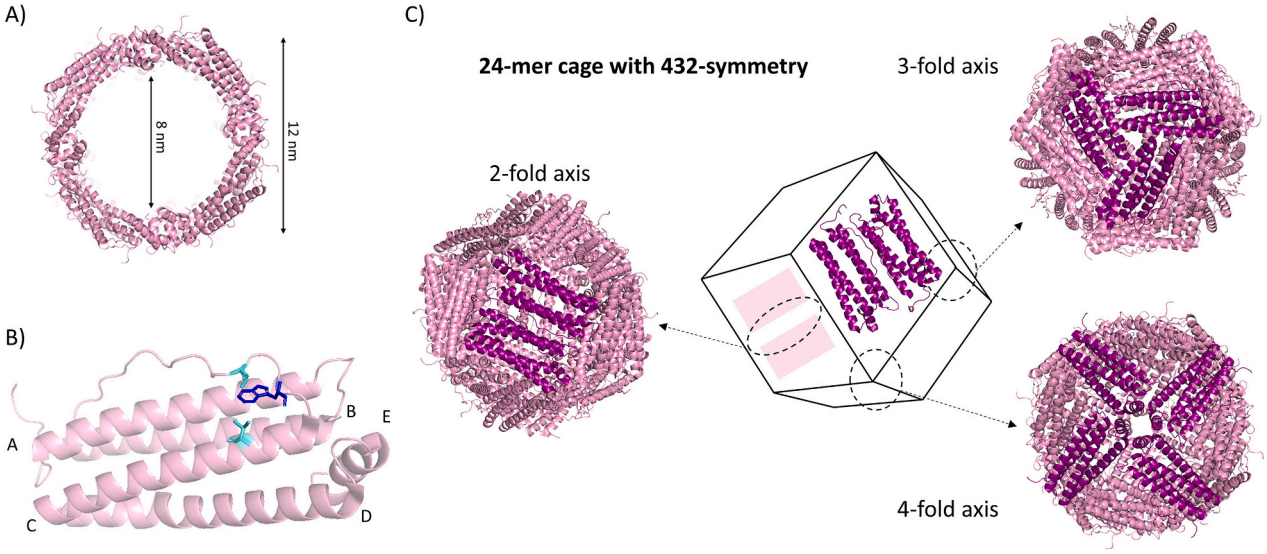

Fig. 1. Nanocage structure of human H-ferritin. A) Cross section of the nanocage showing the large inner cavity. The cage architecture derives from the self-assembly of 24 subunits. (B) Cartoon structure of the H subunit: 4 long-antiparallel α-helices (named A-D), forming a bundle, with a 5th short C-terminal helix (named E), tilted of about 60° with respect to the bundle axis and a solvent exposed loop connecting B and C helices (named BC loop). Each subunit contains a single Trp (W93) highlighted as blue sticks. C90 and C102 are shown in cyan sticks. C) The nanocage is highly symmetric (O- or 432-symmetry). At the 4-fold axes, four subunits come in contact generating six C4-hydrophobic channels; at the 3-fold axes, three subunits encounter, forming eight C3-hydrophilic channels; both channel types connect the external bulk with the inner cavity. At the 2-fold axes, two antiparallel subunits interact (head to tail orientation), with the BC loops along the C2 axis. Drawn using Pymol software and PDB file 4Y08. (For interpretation of the references to colour in this figure legend, the reader is referred to the web version of this article.)

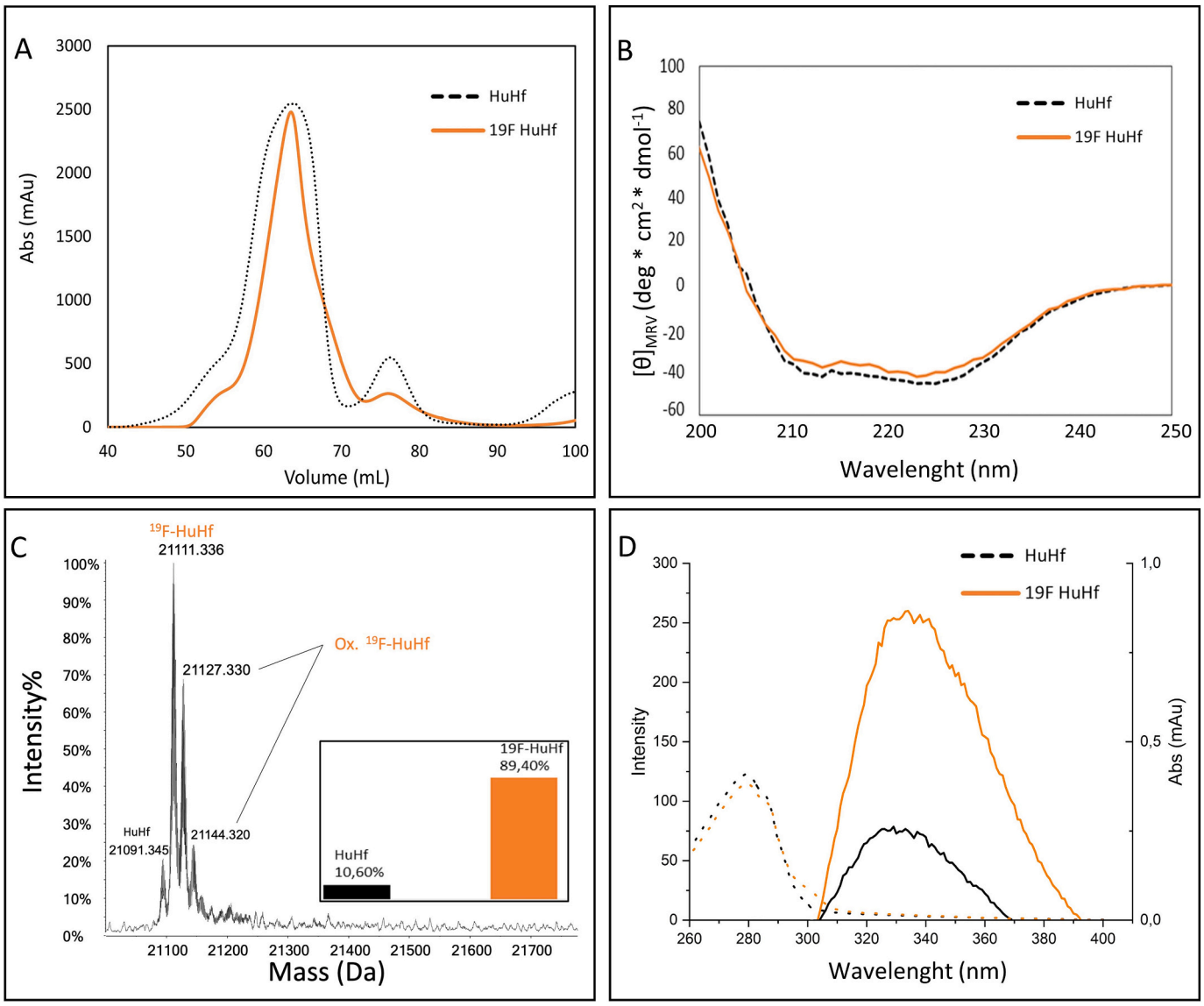

Fig. 2. Characterization of ^{19}F-HuHf. A) Size exclusion chromatography analysis of ^{19}F-HuHf (orange trace) and WT HuHf (black trace). B) Circular dichroism spectra of ^{19}F-HuHf (orange trace) and WT HuHf (black trace). C) Deconvoluted ESI MS spectrum of the purified ^{19}F-HuHf 5×10^{-6} M in 20 mM ammonium acetate solution at pH 6.8, 1% *v*/v of formic acid added just before infusion. Consistently with what reported for the WT [20], the ^{19}F-HuHf monomer is present also in two oxidized forms (see **Fig. S1**); in the inset the percentage of ^{19}F-HuHf subunits and the WT HuHf subunits is shown. D) Combined UV–visible absorbance (λ_{exc} = 280 nm; HuHf and ^{19}F-HuHf 1 μM in 20 mM TRIS, pH 7.5) and fluorescence emission-spectra of ^{19}F-HuHf (λ_{em} = 334 nm, orange trace) and WT HuHf (λ_{em} = 327 nm, black trace), 4 μM/cage in 20 mM TRIS pH 7.5, with 295 nm excitation emission.

ppm vs. ~12 ppm for ^{1}H) [30]. Literature examples [31–35] report chemical shift changes in the range between 0.1 and 1.5 ppm for both protein-protein and protein-small molecules interactions. Despite the very large linewidth of the ^{19}F NMR signal of HuHf, we expect to monitor shift ≥0.2 ppm (as demonstrated in the simulation of **Fig. S3**). Here, we provide a proof of concept that can be considered a prototype for further studies aimed at monitoring the human H ferritin-mediated delivery of metal-based drugs. To this aim we incubated ^{19}F-HuHf with Thimerosal, which contains a mercury(II) ion coordinated to a thiolate and an ethyl group (**Fig. S4**); in the presence of Cys residues, it can bind to the protein as ethylmercury. Human H ferritin contains two solvent exposed Cys (C90 and C102), both in the proximity of Trp93 (Fig. 1B), and addition of stoichiometric amounts of Thimerosal causes the partial formation of a HuHf-ethylmercury adduct with an increment of 229 Da, as monitored by ESI-MS. In solution, we observe two distinct ^{19}F NMR signals for the free and bound HuHf, consistently with a slow exchange regime on the ^{19}F chemical shift time scale (Fig. 3B), which differ for >1 ppm. With the 1:1 ratio we can estimate the presence of about 37% of the bound form by NMR, which compares well with the 36% evaluated by ESI-MS.

Additionally, the absence of any background ^{19}F in biological samples makes ^{19}F-HuHF visible in complex mixtures, including cells lysates (as demonstrated by others for different proteins [35,36]). Here we show that 5 μM cage in a cell lysate provides a peak that in terms of shift, linewidth, and S/N is comparable to that in solution at the same concentration (**Fig. S5**).

On the basis of these two examples, we can anticipate that ^{19}F NMR of ^{19}F-HuHf will be a useful tool in characterizing the cellular uptake of ferritin-based nanocarriers and to monitor the release of metallodrugs bound to the cage.

Another focal aspect of our study is the comparison of ^{19}F vs. ^{13}C labelling of ferritin for NMR purposes. The production of uniformly labeled ^{13}C ferritin is relatively easy [21–26] but, in order to overcome the problem of short T_2 associated with slow molecular tumbling in

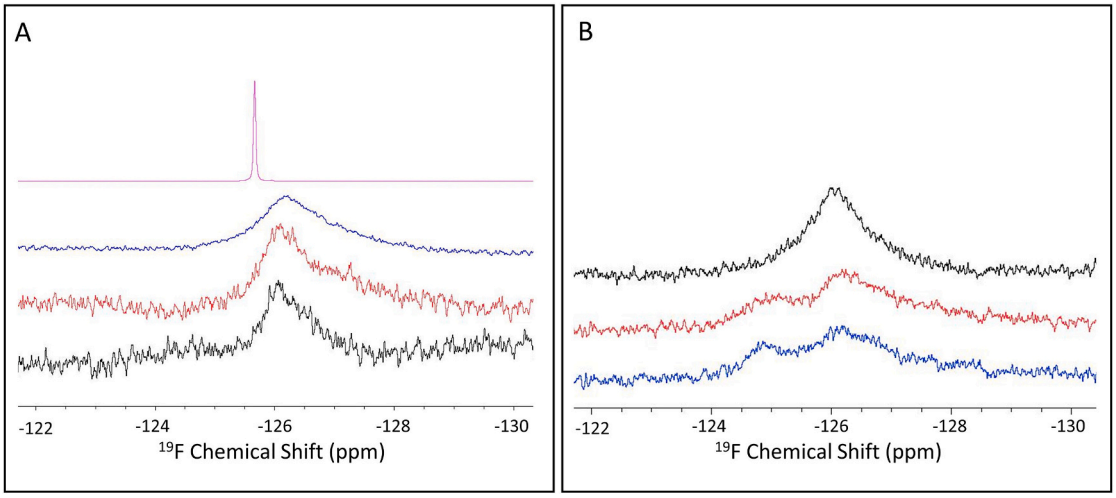

Fig. 3. ^{19}F NMR spectra recorded at 14.1 T and 298 K of A) 5-fluoroindole at 3.6 mM (top pink trace) and ^{19}F-HuHf at different concentrations: 167 μM cage (i.e 3.61 mM of ^{19}F) with 1 k scans corresponding to an acquisition time of 1 h, blue trace; 10 μM cage (i.e. 216 μM of ^{19}F) with 16 k scans, red trace; 5 μM cage (i.e. 108 μM of ^{19}F), 25 k scans, black trace; B) ^{19}F-HuHf 60 μM cage (i.e. 1.4 mM of ^{19}F) with 2 k scans corresponding to an acquisition time of 2 h, alone (black trace) and after 3 h of incubation with Thimerosal (red and blue traces: 1:1 and 1:2 with respect to the ferritin subunit, respectively). The chemical shift values are −124.84 and −126.12 ppm for the bound and free forms, respectively, with ^{19}F chemical shifts referenced to trifluoroacetic acid as an external standard (0 ppm). (For interpretation of the references to colour in this figure legend, the reader is referred to the web version of this article.)

solution, it should be coupled to perdeuteration, thus making NMR samples extremely costly. It has, however, the great advantage of providing atomic resolution information on all protein side chains (with some limitations on the aromatic residues) [21–23]. Conversely, ^{13}C chemical shift is not particularly sensitive to conformational or micro-environmental properties, so ^{13}C-based chemical shift perturbation mapping is not the best approach for structural analyses. Instead, the ^{19}F spectrum here reported was acquired on a fully protonated background (without ^{1}H saturation). As a drawback, it only monitors a given residue on each subunit, but it seems to be a sensitive reporter of the local changes. The ability to detect signals down to a concentration of 5 μM (a lower limit that could be improved with the use of dedicated probes) even in crowded solutions (**Fig. S5**) paves the way to the use of the ^{19}F signal as the reporter of the presence of up-taken ferritin in cell lysates (or extracts from sub-cellular compartments) in studies aimed at characterizing the delivery of drugs mediated by HuHf, a context where ^{13}C-labeling is useless due to strong background signal for the natural abundance (1.1%) [37].

Finally, the approach here proposed for HuHf could be extended to the homopolymeric human L ferritin, which can be used as an alternative nanocarrier to be internalized by those tumor cells overexpressing Scavenger receptor class A member 5 (SCARA5) [38]; human L-ferritin also has a Trp at the corresponding position in its subunits [39,40]. Similar considerations apply to any other Trp-containing ferritin.

A postscript about Ann

I met Ann Walker as she was one of the pioneers in the field of paramagnetic NMR who belonged to the generation and international group of colleagues with whom Ivano Bertini had close scientific and personal relationships. Ann was a constant presence at the many congresses on bioinorganic NMR organized in Florence in “Ivano’s era” and visited our laboratory several times. She was the recipient of the 2001 Luigi Sacconi Medal of the Inorganic Chemistry Division of the Italian Chemical Society, with Ivano as one of the main supporters of her candidacy.

Thanks to these several opportunities of encounter and for the joint interest in NMR of heme proteins, I had the chance to develop a personal relationship with Ann. She kindly invited me to visit her lab at the University of Arizona, and, simultaneously, she warmly hosted me together with my family at her home in the summer of 2010 and guided us around in the Sonoran Desert. Together with Ivano, I met Ann in person for the last time for the celebration of her 70th birthday organized at the ACS 241st National Meeting in Anaheim in March 2011.

Reflecting on the story of our friendship, I think this is an example of how common scientific interests can lay the foundations for intergenerational ties that go beyond geographical borders.

CRediT authorship contribution statement

Lucrezia Cosottini: Methodology, Investigation, Writing – original draft. **Stefano Zineddu:** Investigation, Writing – review & editing. **Lara Massai:** Investigation, Writing – review & editing. **Veronica Ghini:** Investigation, Writing – original draft. **Paola Turano:** Conceptualization, Writing – original draft, Supervision.

Declaration of Competing Interest

The authors declare that they have no known competing financial interests or personal relationships that could have appeared to influence the work reported in this paper.

Data availability

Data will be made available on request.

Acknowledgments

We acknowledge the support and the use of resources of Instruct-ERIC, a landmark ESFRI project, and specifically the CERM/CIRMMP Italy Centre.

Appendix A. Supplementary data

Supplementary data to this article can be found online at https://doi.org/10.1016/j.jinorgbio.2023.112236.

References

[1] A.M. Gronenborn, Small, but powerful and attractive: 19F in biomolecular NMR, Structure. 30 (2022) 6–14, https://doi.org/10.1016/j.str.2021.09.009.

[2] R.R. Crichton, J.-P. Declercq, X-ray structures of ferritins and related proteins, Biochim. Biophys. Acta Gen. Subj. 1800 (2010) 706–718, https://doi.org/10.1016/j.bbagen.2010.03.019.

[3] C. Pozzi, F. Di Pisa, C. Bernacchioni, S. Ciambellotti, P. Turano, S. Mangani, Iron binding to human heavy-chain ferritin, Acta Cryst D. 71 (2015) 1909–1920, https://doi.org/10.1107/S1399004715013073.

[4] L.C. Montemiglio, C. Testi, P. Ceci, E. Falvo, M. Pitea, C. Savino, A. Arcovito, G. Peruzzi, P. Baiocco, F. Mancia, A. Boffi, A. Des Georges, B. Vallone, Cryo-EM structure of the human ferritin-transferrin receptor 1 complex, Nat. Commun. 10 (2019) 1121, https://doi.org/10.1038/s41467-019-09098-w.

[5] L. Li, C.J. Fang, J.C. Ryan, E.C. Niemi, J.A. Lebrón, P.J. Björkman, H. Arase, F. M. Torti, S.V. Torti, M.C. Nakamura, W.E. Seaman, Binding and uptake of H-ferritin are mediated by human transferrin receptor-1, Proc. Natl. Acad. Sci. U. S. A. 107 (2010) 3505–3510, https://doi.org/10.1073/pnas.0913192107.

[6] J. Zhang, D. Cheng, J. He, J. Hong, C. Yuan, M. Liang, Cargo loading within ferritin nanocages in preparation for tumor-targeted delivery, Nat. Protoc. 16 (2021) 4878–4896, https://doi.org/10.1038/s41596-021-00602-5.

[7] N. Song, J. Zhang, J. Zhai, J. Hong, C. Yuan, M. Liang, Ferritin: a multifunctional Nanoplatform for biological detection, imaging diagnosis, and drug delivery, Acc. Chem. Res. 54 (2021) 3313–3325, https://doi.org/10.1021/acs.accounts.1c00267.

[8] L. Conti, S. Ciambellotti, G.E. Giacomazzo, V. Ghini, L. Cosottini, E. Puliti, M. Severi, E. Fratini, F. Cencetti, P. Bruni, B. Valtancoli, C. Giorgi, P. Turano, Ferritin nanocomposites for the selective delivery of photosensitizing ruthenium-polypyridyl compounds to cancer cells, Inorg. Chem. Front. 9 (2022) 1070–1081, https://doi.org/10.1039/D1QI01268A.

[9] J.C. Cutrin, S.G. Crich, D. Burghelea, W. Dastrù, S. Aime, Curcumin/Gd loaded apoferritin: a novel "Theranostic" agent to prevent hepatocellular damage in toxic induced acute hepatitis, Mol. Pharm. 10 (2013) 2079–2085, https://doi.org/10.1021/mp3006177.

[10] J. Zhang, Z. Zhang, M. Jiang, S. Li, H. Yuan, H. Sun, F. Yang, H. Liang, Developing a novel gold(III) agent to treat glioma based on the unique properties of Apoferritin nanoparticles: inducing lethal autophagy and apoptosis, J. Med. Chem. 63 (2020) 13695–13708, https://doi.org/10.1021/acs.jmedchem.0c01257.

[11] R. Lucignano, A. Pratesi, P. Imbimbo, D.M. Monti, D. Picone, L. Messori, G. Ferraro, A. Merlino, Evaluation of Auranofin loading within ferritin Nanocages, Int. J. Mol. Sci. 23 (2022) 14162, https://doi.org/10.3390/ijms232214162.

[12] E. Ravera, S. Ciambellotti, L. Cerofolini, T. Martelli, T. Kozyreva, C. Bernacchioni, S. Giuntini, M. Fragai, P. Turano, C. Luchinat, Solid-state NMR of PEGylated proteins, Angew. Chem. Int. Ed. Eng. 55 (2016) 2446–2449, https://doi.org/10.1002/anie.201510148.

[13] Z. Wang, H. Gao, Y. Zhang, G. Liu, G. Niu, X. Chen, Functional ferritin nanoparticles for biomedical applications, Front. Chem. Sci. Eng. 11 (2017) 633–646, https://doi.org/10.1007/s11705-017-1620-8.

[14] J. Zemsky, E. Rusinova, Y. Nemerson, L.A. Luck, J.B. Ross, Probing local environments of tryptophan residues in proteins: comparison of 19F nuclear magnetic resonance results with the intrinsic fluorescence of soluble human tissue factor, Proteins. 37 (1999) 709–716.

[15] M. Leone, R.A. Rodriguez-Mias, M. Pellecchia, Selective incorporation of 19F-labeled Trp side chains for NMR-spectroscopy-based ligand-protein interaction studies, ChemBioChem. 4 (2003) 649–650, https://doi.org/10.1002/cbic.200300597.

[16] P.D. Hempstead, S.J. Yewdall, A.R. Fernie, D.M. Lawson, P.J. Artymiuk, D.W. Rice, G.C. Ford, P.M. Harrison, Comparison of the three-dimensional structures of recombinant human H and horse L ferritins at high resolution 1 1Edited by R, Huber, J. Mol. Biol. 268 (1997) 424–448, https://doi.org/10.1006/jmbi.1997.0970.

[17] R. Curtis-Marof, D. Doko, M.L. Rowe, K.L. Richards, R.A. Williamson, M.J. Howard, ^{19}F NMR spectroscopy monitors ligand binding to recombinantly fluorine-labelled **b** ′ **x** from human protein disulphide isomerase (hPDI), Org. Biomol. Chem. 12 (2014) 3808–3812, https://doi.org/10.1039/C4OB00699B.

[18] A.K. Urick, L.M.L. Hawk, M.K. Cassel, N.K. Mishra, S. Liu, N. Adhikari, W. Zhang, C.O. dos Santos, J.L. Hall, W.C.K. Pomerantz, Dual screening of BPTF and Brd4 using protein-observed fluorine NMR uncovers new Bromodomain probe molecules, ACS Chem. Biol. 10 (2015) 2246–2256, https://doi.org/10.1021/acschembio.5b00483.

[19] C. Bernacchioni, V. Ghini, E.C. Theil, P. Turano, Modulating the permeability of ferritin channels, RSC Adv. 6 (2016) 21219–21227, https://doi.org/10.1039/C5RA25056K.

[20] L. Massai, S. Ciambellotti, L. Cosottini, L. Messori, P. Turano, A. Pratesi, Direct detection of iron clusters in L ferritins through ESI-MS experiments, Dalton Trans. 50 (2021) 16464–16467, https://doi.org/10.1039/d1dt03106f.

[21] M. Matzapetakis, P. Turano, E.C. Theil, I. Bertini, 13C- 13C NOESY spectra of a 480 kDa protein: solution NMR of ferritin, J. Biomol. NMR 38 (2007) 237–242, https://doi.org/10.1007/s10858-007-9163-9.

[22] P. Turano, D. Lalli, I.C. Felli, E.C. Theil, I. Bertini, NMR reveals pathway for ferric mineral precursors to the central cavity of ferritin, Proc. Natl. Acad. Sci. U. S. A. 107 (2010) 545–550, https://doi.org/10.1073/pnas.0908082106.

[23] D. Lalli, P. Turano, Solution and solid state NMR approaches to draw iron pathways in the ferritin nanocage, Acc. Chem. Res. 46 (2013) 2676–2685, https://doi.org/10.1021/ar4000983.

[24] M. Piccioli, P. Turano, Transient iron coordination sites in proteins: exploiting the dual nature of paramagnetic NMR, Coord. Chem. Rev. 284 (2015) 313–328, https://doi.org/10.1016/j.ccr.2014.05.007.

[25] W. Bermel, I. Bertini, I.C. Felli, M. Matzapetakis, R. Pierattelli, E.C. Theil, P. Turano, A method for C(alpha) direct-detection in protonless NMR, J. Magn. Reson. 188 (2007) 301–310, https://doi.org/10.1016/j.jmr.2007.07.004.

[26] V. Ghini, S. Chevance, P. Turano, About the use of 13C-13C NOESY in bioinorganic chemistry, J. Inorg. Biochem. 192 (2019) 25–32, https://doi.org/10.1016/j.jinorgbio.2018.12.006.

[27] S.M. Twine, A.G. Szabo, [4] Fluorescent amino acid analogs, in: Methods in Enzymology, Elsevier, 2003, pp. 104–127, https://doi.org/10.1016/S0076-6879(03)60108-4.

[28] G.R. Winkler, S.B. Harkins, J.C. Lee, H.B. Gray, α-Synuclein structures probed by 5-Fluorotryptophan fluorescence and 19F NMR spectroscopy, J. Phys. Chem. B 110 (2006) 7058–7061, https://doi.org/10.1021/jp060043n.

[29] J. Xu, B. Chen, P. Callis, P.L. Muiño, H. Rozeboom, J. Broos, D. Toptygin, L. Brand, J.R. Knutson, Picosecond fluorescence dynamics of tryptophan and 5-Fluorotryptophan in monellin: slow water–protein relaxation unmasked, J. Phys. Chem. B 119 (2015) 4230–4239, https://doi.org/10.1021/acs.jpcb.5b01651.

[30] C.M. Pfefferkorn, J.C. Lee, 5-fluoro-D,L-tryptophan as a dual NMR and fluorescent probe of α-synuclein, Methods Mol. Biol. 895 (2012) 197–209, https://doi.org/10.1007/978-1-61779-927-3_14.

[31] D. Li, Y. Zhang, Y. He, C. Zhang, J. Wang, Y. Xiong, L. Zhang, Y. Liu, P. Shi, C. Tian, Protein-protein interaction analysis in crude bacterial lysates using combinational method of 19F site-specific incorporation and 19F NMR, protein, Cell. 8 (2017) 149–154, https://doi.org/10.1007/s13238-016-0336-8.

[32] S.S. Stadmiller, J.S. Aguilar, C.A. Waudby, G.J. Pielak, Rapid quantification of protein-ligand binding via 19F NMR Lineshape analysis, Biophys. J. 118 (2020) 2537–2548, https://doi.org/10.1016/j.bpj.2020.03.031.

[33] A. Divakaran, S.E. Kirberger, W.C.K. Pomerantz, SAR by (protein-observed) ^{19} F NMR, Acc. Chem. Res. 52 (2019) 3407–3418, https://doi.org/10.1021/acs.accounts.9b00377.

[34] Y. Hattori, D. Heidenreich, Y. Ono, T. Sugiki, K. Yokoyama, E. Suzuki, T. Fujiwara, C. Kojima, Protein 19F-labeling using transglutaminase for the NMR study of intermolecular interactions, J. Biomol. NMR 68 (2017) 271–279, https://doi.org/10.1007/s10858-017-0125-6.

[35] L.B.T. Pham, A. Costantino, L. Barbieri, V. Calderone, E. Luchinat, L. Banci, Direct expression of fluorinated proteins in human cells for ^{19} F in-cell NMR spectroscopy, J. Am. Chem. Soc. 145 (2023) 1389–1399, https://doi.org/10.1021/jacs.2c12086.

[36] H. Welte, M. Kovermann, Insights into protein stability in cell lysate by 19F NMR spectroscopy, ChemBioChem. 21 (2020) 3575–3579, https://doi.org/10.1002/cbic.202000413.

[37] A.Y. Maldonado, D.S. Burz, A. Shekhtman, In-cell NMR spectroscopy, Prog. Nucl. Magn. Reson. Spectrosc. 59 (2011) 197–212, https://doi.org/10.1016/j.pnmrs.2010.11.002.

[38] J.Y. Li, N. Paragas, R.M. Ned, A. Qiu, M. Viltard, T. Leete, I.R. Drexler, X. Chen, S. Sanna-Cherchi, F. Mohammed, D. Williams, C.S. Lin, K.M. Schmidt-Ott, N. C. Andrews, J. Barasch, Scara5 is a ferritin receptor mediating non-transferrin Iron delivery, Dev. Cell 16 (2009) 35–46, https://doi.org/10.1016/j.devcel.2008.12.002.

[39] S. Ciambellotti, C. Pozzi, S. Mangani, P. Turano, Iron biomineral growth from the initial nucleation seed in L-ferritin, Chem. Eur. J. 26 (2020) 5770–5773, https://doi.org/10.1002/chem.202000064.

[40] C. Pozzi, S. Ciambellotti, C. Bernacchioni, F. Di Pisa, S. Mangani, P. Turano, Chemistry at the protein–mineral interface in L-ferritin assists the assembly of a functional (μ^3-oxo)Tris[(μ^2-peroxo)] triiron(III) cluster, Proc. Natl. Acad. Sci. U. S. A. 114 (2017) 2580–2585, https://doi.org/10.1073/pnas.1614302114.